Interpretation of Testing Results on TRULINE Composite Wall Sections

Phase 1 Report

Presented to

Formtech Enterprises, Inc./ TRULINE

126 Ben Burton Circle

Bogart, Georgia 30622

by

Ensoft, Inc.

3003 Howard Lane

Austin, Texas 78728

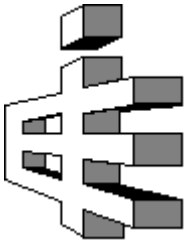

June 6, 2012

Table of Contents

List of Figures

Introduction

The subject of this report is the analysis of the tests performed on four composite Truline wall sections.

Description of Test Specimens

The four test specimens were constructed using Truline PVC filled with reinforced concrete. The details of the four test specimens are described in the following paragraphs.

Specimen 1 was composed of two Series 1200 PVC sections filled with reinforced concrete. Each PVC section was divided into two cells, so this specimen has a total of four cells. This test specimen had a nominal dimension of 36 inches in width and 12 inches in depth. The concrete had a measured compressive strength of 3,020 psi. The reinforcement was composed of two No. 8 bars in each cell for a total of eight bars in the specimen. The yield stress of the No. 8 bars had a yield stress of 63,600 psi.

Specimen 2 was composed of three Series 800 PVC sections filled with reinforced concrete. Each PVC section was divided into two cells, so this specimen has a total of six cells. This test specimen had a nominal dimension of 36 inches in width and 8 inches in depth. The concrete had a measured compressive strength of 3,020 psi. The reinforcement was composed of two No. 5 bars in each cell for a total of twelve bars in the specimen. The yield stress of the No. 5 bars had a yield stress of 67,600 psi. Three-inch diameter holes were drilled through the web of the PVC on 12-inch centers to enhance flow of fluid concrete between cells during construction.

Specimen 3 was composed of three Series 800 PVC sections filled with reinforced concrete. Each PVC section was divided into two cells, so this specimen has a total of six cells. This test specimen had a nominal dimension of 36 inches in width and 8 inches in depth. The concrete had a measured compressive strength of 3,020 psi. The reinforcement was composed of one No. 5 bars in each PVC section (one bar in every other cell for a total of three bars in the specimen). The yield stress of the No. 5 bars had a yield stress of 67,600 psi. The bars were positioned to be on the tension side of the specimen during testing.

Specimen 4 is nearly identical to Specimen 2, except that the 3-inch diameter holes in the webs between cells were eliminated.

Testing Procedures

Testing Arrangement

The arrangement for testing is shown in Figure 1. In this arrangement, equal loads are applied to the ends of the test specimen and the two central support points are equal distances from the two ends. The length of the test specimen is 144 inches and the two central support points are 50 inches apart. Beam deflections are measured at the mid-point of the specimen on the bottom of the specimen.

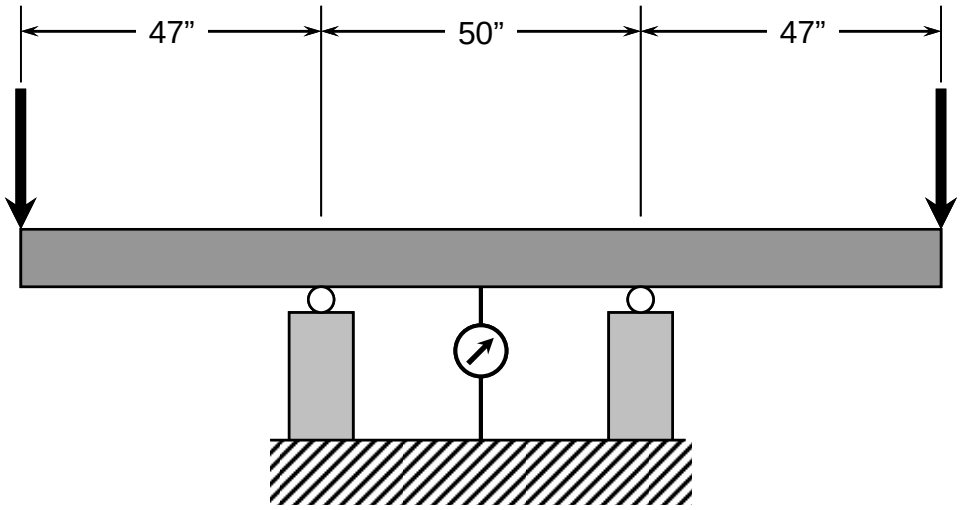

Figure 1 Testing Arrangement

Shear Force and Bending Moment Diagrams

The shear and moment diagrams for the test specimens are shown in Figure 2.

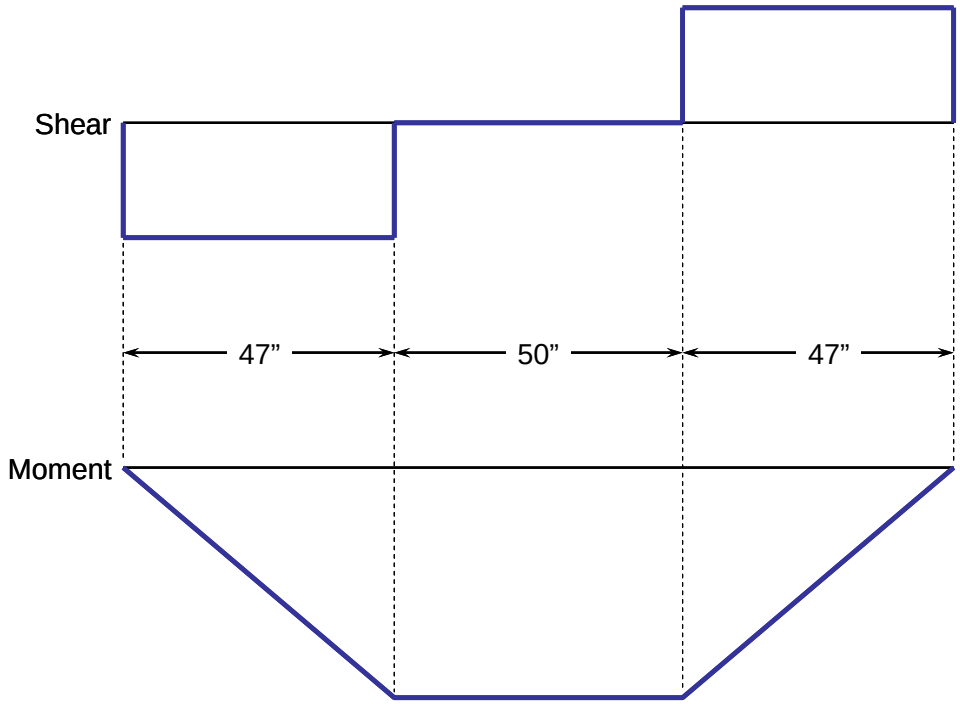

Figure 2 Shear Force and Bending Moment Diagrams for Test Specimens

The noteworthy feature of this testing arrangement is the zone of pure moment between the two central support points. Theoretically, a beam subjected to pure moment deforms as a circular arc. This permits the evaluation of bending curvature from relatively simple measurements of deformation.

Predictions of Test Performance

Prediction of test performance for the as-built test specimens was made using LPile 2012. The mechanistic analysis features for moment-curvature computations are described in the LPile 2012 Technical Manual and are summarized in Appendix B of this report.

The test predictions were made by first computing the moment-curvature behavior using the as-built geometries and material properties. The corresponding center-point rise versus applied end-forces were made using the equations presented in the following section of this report.

The predicted performance curves are included in the Figures 4 through 11.

Methods of Analysis

The methods of analysis are based on the geometry of a circular arc. The following paragraphs present the geometry and derivation of the expression to compute bending curvature from the rise of the center-point of a test specimen.

The derivation of the expression to compute bending curvature is based on the geometry of a circular segment. The Figure below shows the geometry and terminology used to describe the center-point rise, *h*, and the spacing of the two central supports, *c*.

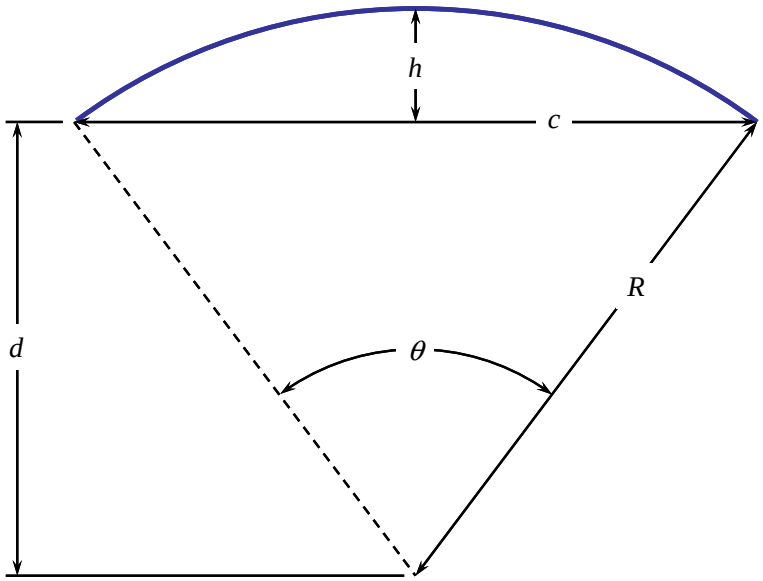

Figure 3 Geometry of Curvature

The following relationships were obtained that relate *h* to *c* from CRC Standard Mathematical Tables, 25th Edition, page 143, Geometry, Sector and Segment of Circle,

$$c = 2R\sin\frac{\theta}{2} = 2d\ \tan\frac{\theta}{2}$$

$$c = 2\sqrt{R^2 - d^2} = \sqrt{4h(2R-h)}$$

The value of curvature, ϕ, is defined as the reciprocal of the radius of curvature, R, or as

$$\phi = \frac{1}{R}$$

Thus, an expression for curvature can be obtained by expressing the radius of curvature to the measured center-point rise. The following is the derivation for this expression.

$$c = \sqrt{4h(2R-h)}$$

$$c^2 = 4h(2R-h)$$

$$2R - h = \frac{c^2}{4h}$$

$$2R = \frac{c^2}{4h} + h$$

$$2R = \frac{c^2 + 4h^2}{4h}$$

$$R = \frac{c^2 + 4h^2}{8h}$$

$$\phi = \frac{1}{R} = \frac{8h}{c^2 + 4h^2}$$

$$\phi = \frac{8h}{c^2 + 4h^2}$$

Test Results

The measurements of center-point rise versus applied bending moment are shown in the Figures 4 through 7. Curve for the predicted performance for as-built properties are also shown in the figures as the curves without symbols.

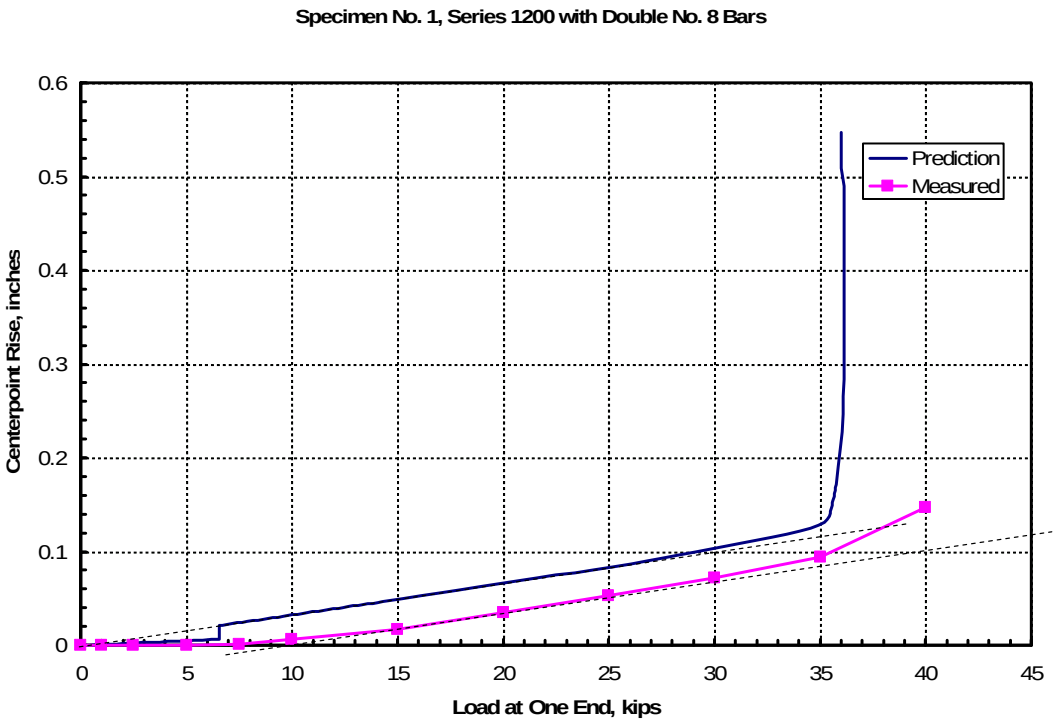

Figure 4 Center-point Rise vs. Applied Bending Moment for Specimen 1

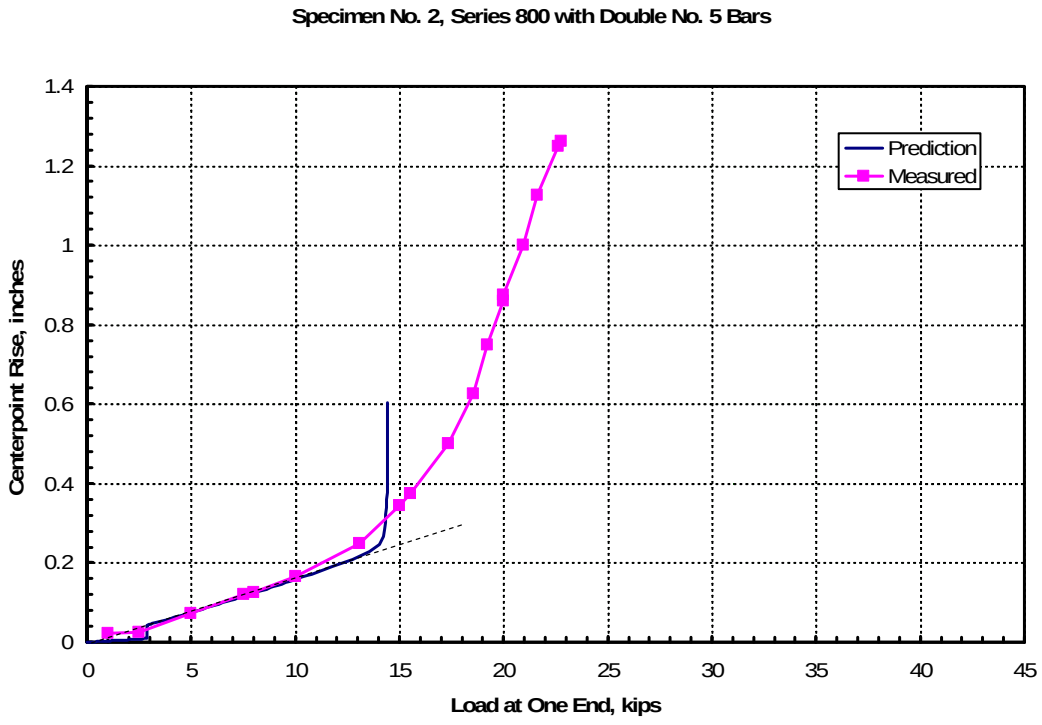

Figure 5 Center-point Rise vs. Applied Bending Moment for Specimen 2

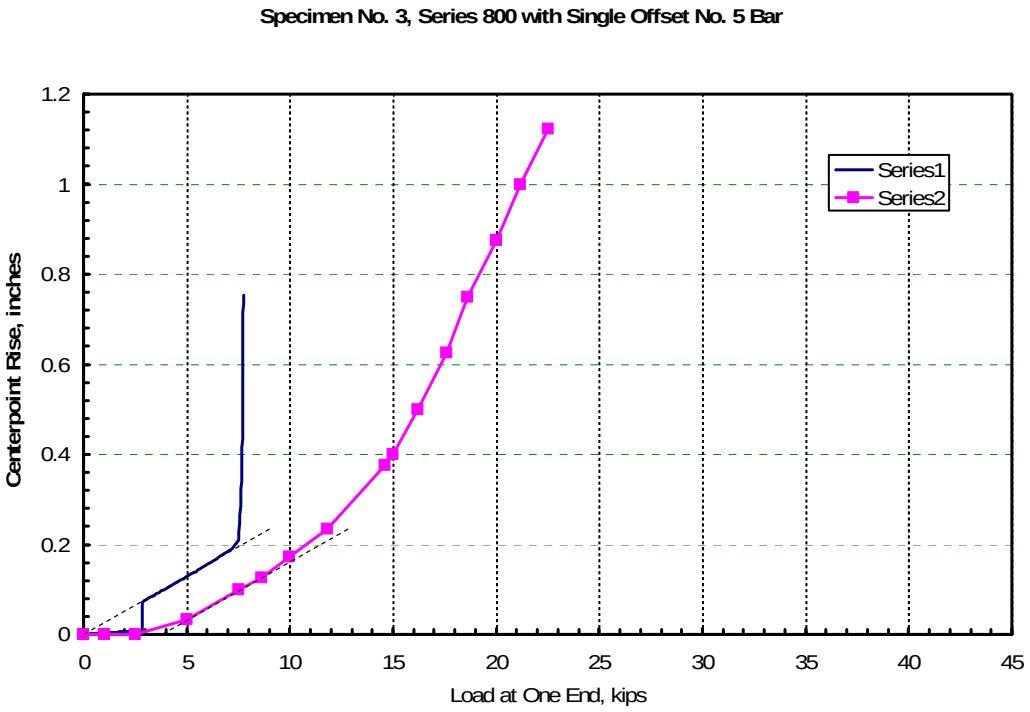

Figure 6 Center-point Rise vs. Applied Bending Moment for Specimen 3

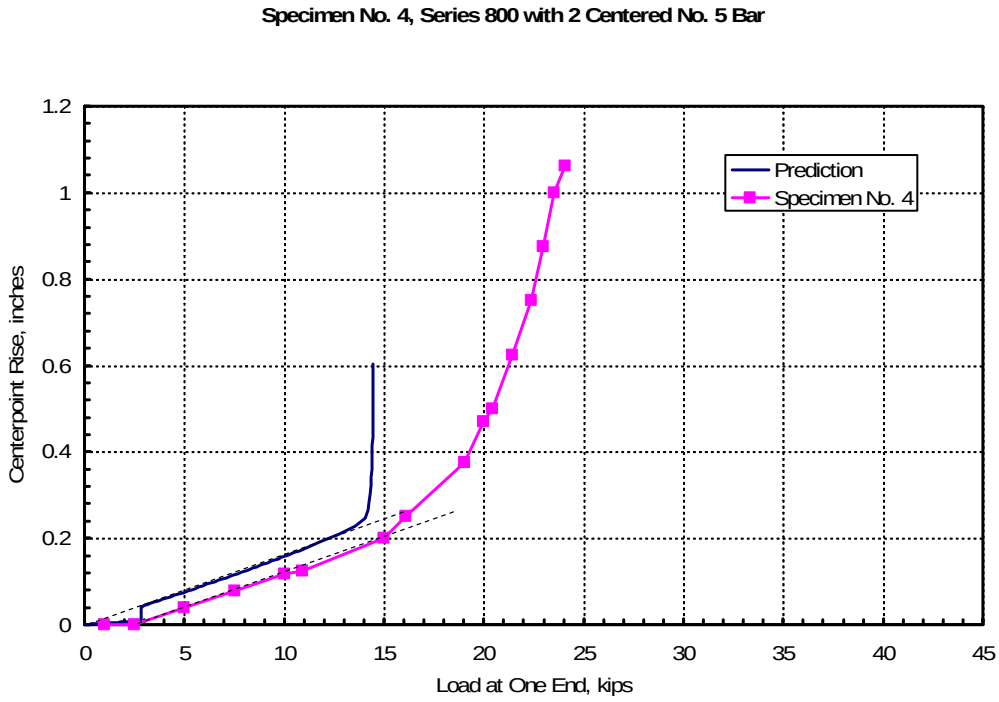

Figure 7 Center-point Rise vs. Applied Bending Moment for Specimen 4

Analysis of Testing Results

The interpreted test results are presented in Figures 8 through 11 as plots of bending moment versus bending curvature.

The predicted curve of performance is indicated by the curve without symbols. Several parts of the predicted curve are labeled in Figure 8 to indicate when the concrete cracks in tension, when the reinforcing steel yields in tension, and when the concrete crushes in compression.

The tangential bending stiffness is indicated by the dashed lines added to the figures. These lines were drawn by first drawing a line from the origin tangent to the predicted cracked-section curve, then making a parallel copy of the first line and placing the copy over the measured curve. In all specimens, the parallel copy closely matched the tangential stiffness of the measured curves.

All specimens exhibited behavior in which the peak moments developed exceeded the failure moments predicted by mechanistic analysis of moment-curvature behavior. This is explained by the development axial stresses higher than the yield stress in the reinforcing bars. The tensile tests performed by Architectural Testing, Inc. found fracture stress values of 109,500 psi for the No. 8 bars (versus a yield stress of 63,600 psi) and of 115,300 psi for the No. 5 bars. This is usually explained by the fact that much reinforcing steel bars available in the United States are made from recycled steel, which typically exhibit higher fracture stresses and reduced ductility than the stress-strain model assumes for reinforcing steel in the mechanistic analysis.

What is important to recognize in the test results is the parallel sections of the predicted and measured curves, as indicated by the note in Figure 8 and also seen in Figures 9, 10, and 11. The parallel curves indicate that the tangential stiffness of the sections can be predicted with reasonable accuracy. This is important because this permits the designing engineer to make computations of the cracked section bending stiffness to be used in design of earth retaining structures using the composite wall sections.

Specimen 2 showed the best match between the predicted and measured curves in the cracked-section behavior below yield. This specimen exhibited a moment capacity higher than predicted due to the high fracture strength of the reinforcing steel.

Comparison of Specimens 2 and 4

Specimens 2 and 4 are similar in structural details and materials, with the addition of 3-inch holes on 12-inch centers to Specimen 4 to aid constructability. The structural performance of the two specimens as designed should be identical. The results for these two specimens are plotted together in Figures 12 and 13.

The two specimens exhibit close to identical stiffness responses in the center-point rise versus applied force graph in Figure 12 and in the moment-curvature graph shown in Figure 13. The purpose of these two graphs is to illustrate that the tangential stiffness of the two test specimens is virtually identical.

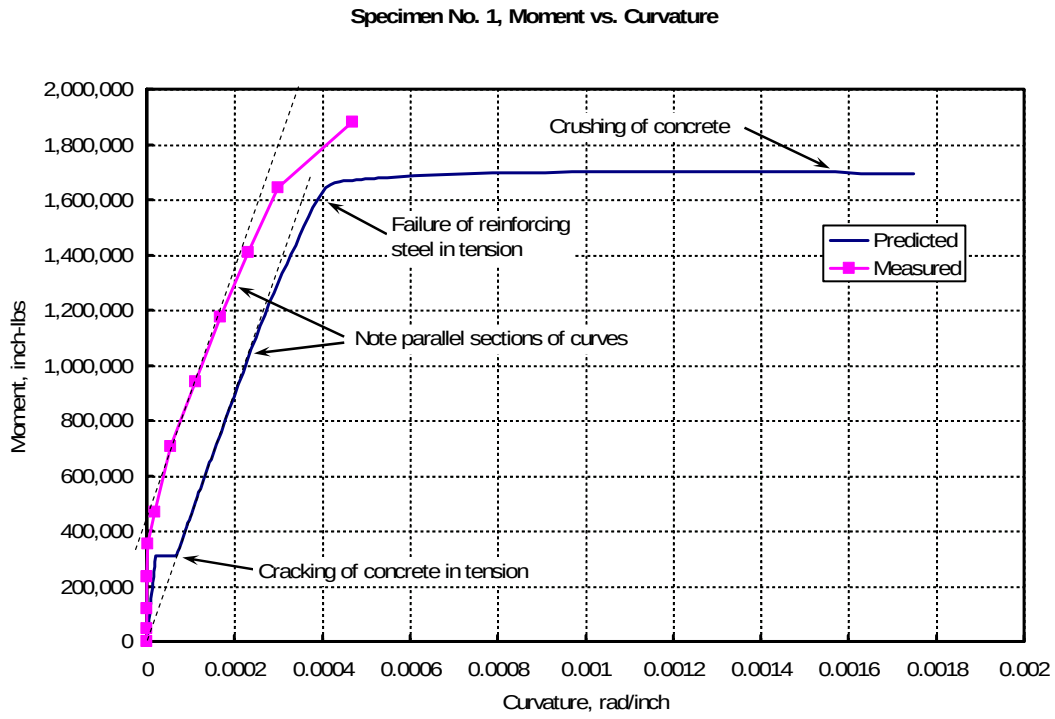

Figure 8 Bending Moment vs. Bending Curvature for Specimen 1

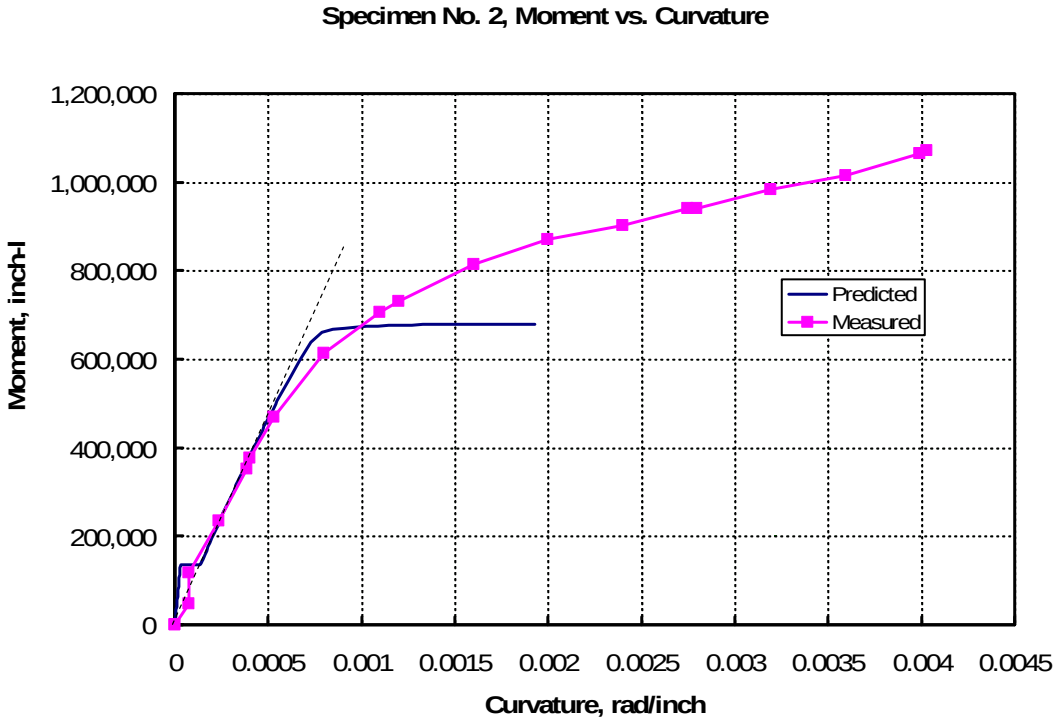

Figure 9 Bending Moment vs. Bending Curvature for Specimen 2

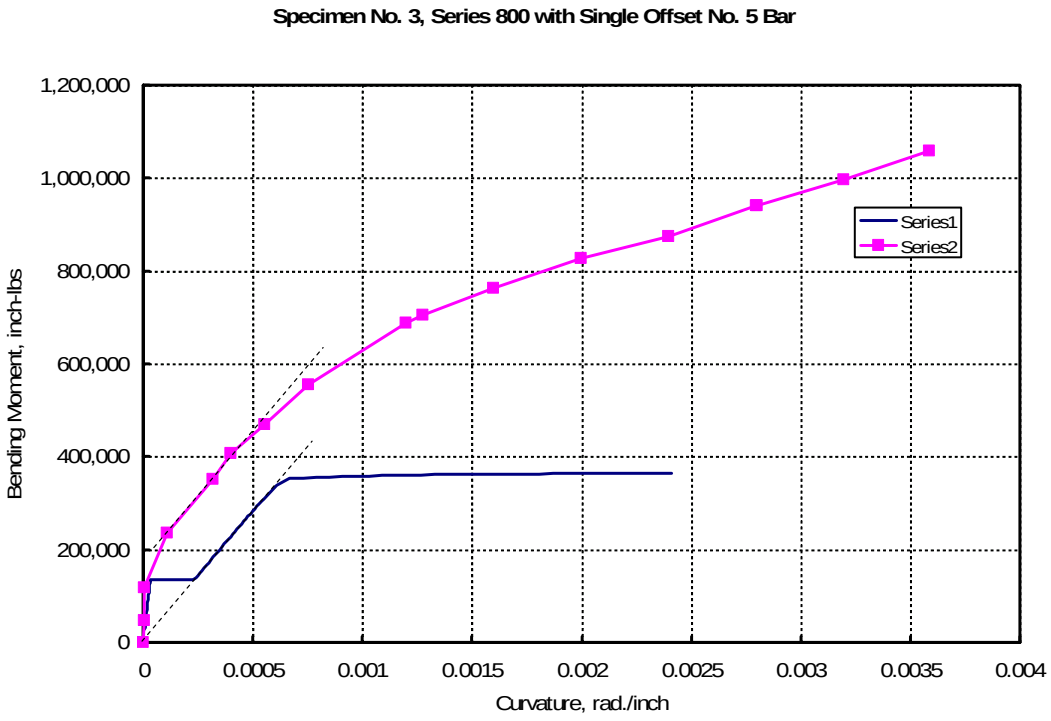

Figure 10 Bending Moment vs. Bending Curvature for Specimen 3

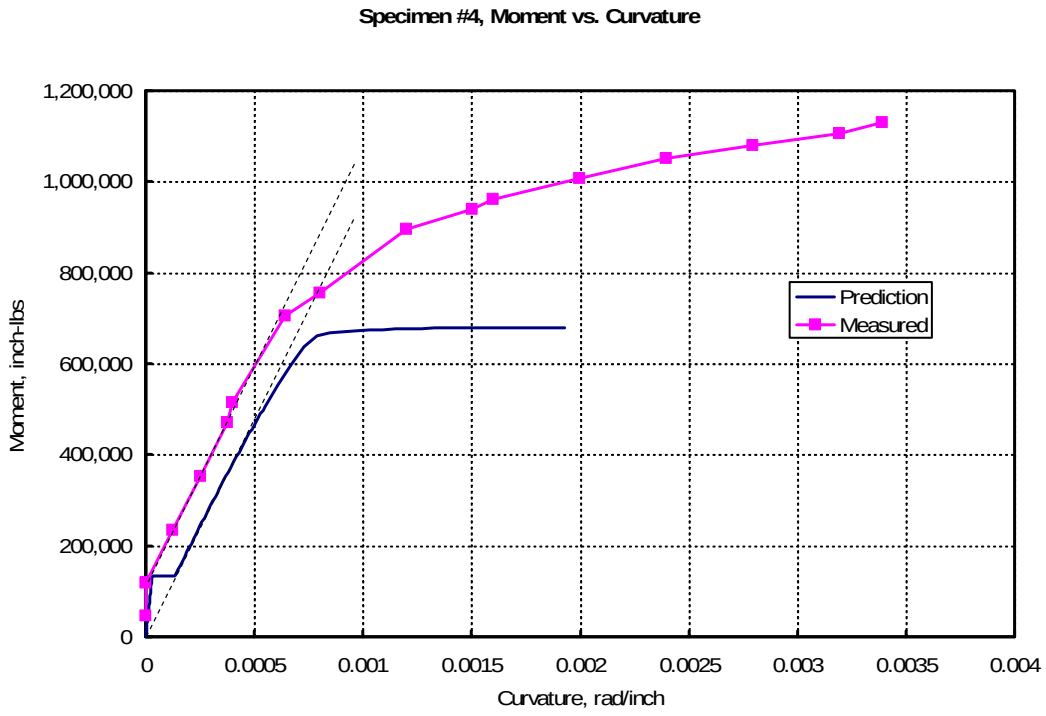

Figure 11 Bending Moment vs. Bending Curvature for Specimen 4

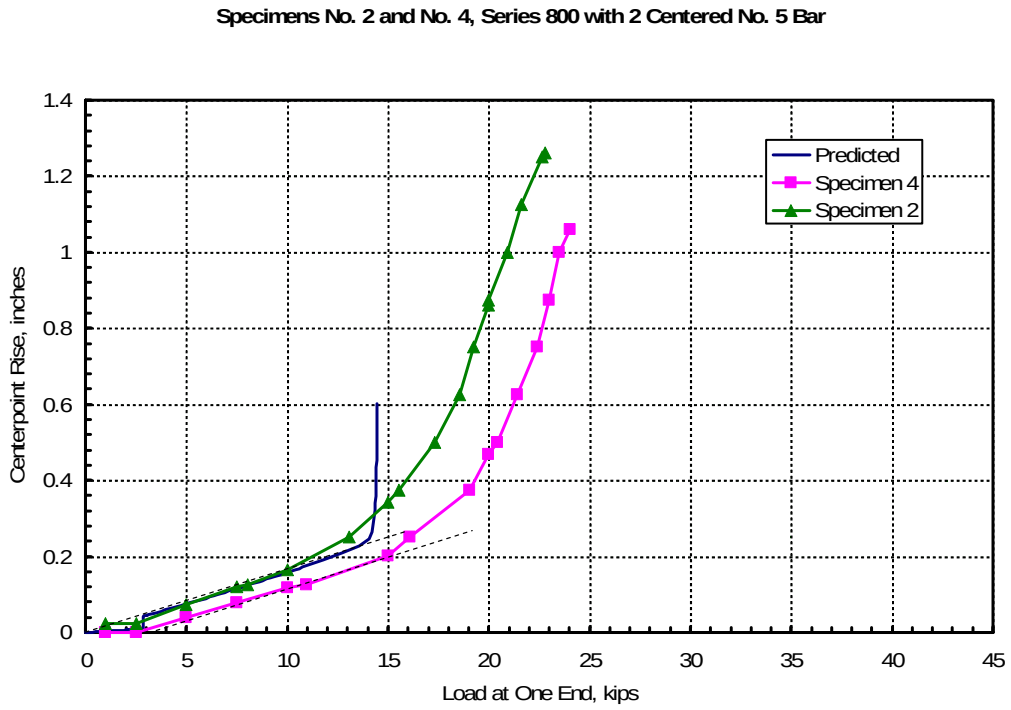

Figure 12 Center-point Rise vs. Applied Bending Moment for Specimens 2 and 4

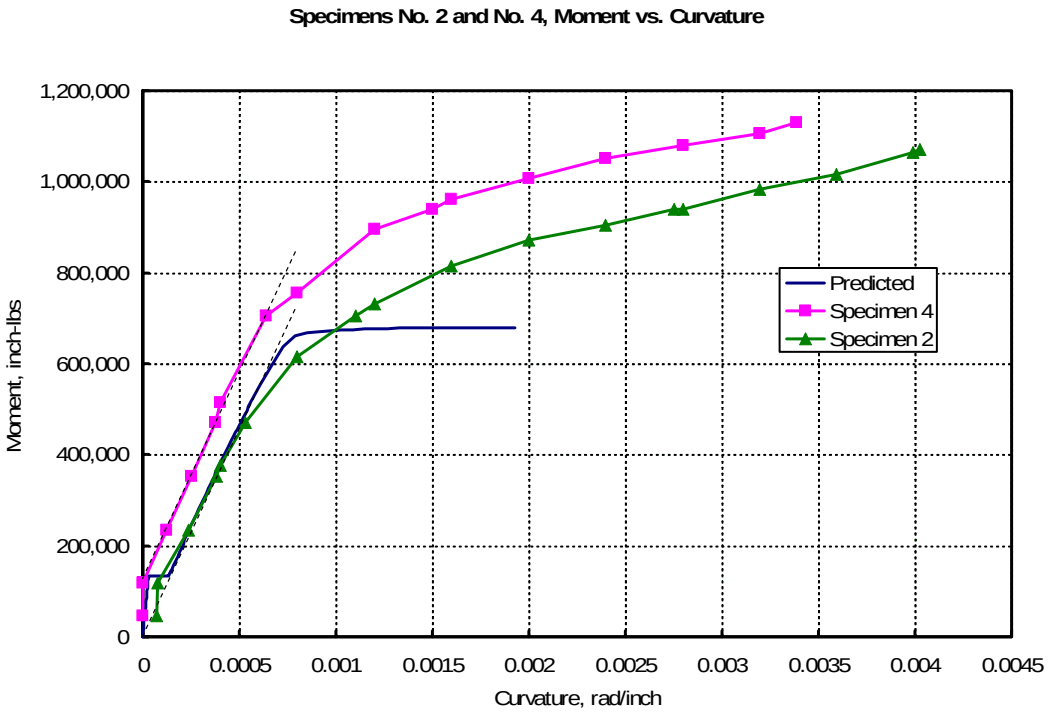

Figure 13 Bending Moment vs. Bending Curvature for Specimens 2 and 4

Conclusions

This report presents an analysis of the test results on bending load tests of composite PVC wall sections utilizing Series 1200 and 800 Truline cast-in-place wall sections.

Predictions of test performance were made using a mechanistic bending analysis in which the non-linear stress-strain curves of the various materials in the wall were considered.

All test specimens exhibited peak moment capacities higher than the predicted values. This is explained by the measured fracture stress in the steel reinforcement being significantly higher than the measured yield stresses.

All test specimens exhibited cracked-section stiffnesses that were a close match with the predictions made by mechanistic analysis. The close match was indicated by the parallel curves in the graphs of moment versus curvature in Figures 8 through 11. The close match in computed and measured stiffness enables designing engineers to use mechanistic computations of bending stiffness of the composite sections.

The responses of Specimens 2 and 4 exhibit virtually identical tangential stiffnesses, as shown in Figures 12 and 13. These results show that computations of bending stiffness of the composite wall sections can be made with a high degree of confidence.

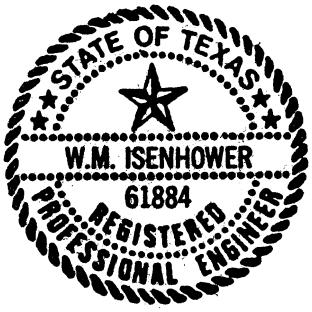

June 6, 2012

William M. Isenhower

William M. Isenhower, Ph.D., P.E.
Project Manager
Ensoft, Inc.

Appendix A

Results of Finite Element Analysis of Elastic Section with Initial Twist

The graph below shows the variation in center-point rise for an elastic beam with an initial twist of 3 degrees over a length of 144 inches. The deflections are across a center-line perpendicular to the long axis of the specimen. The modeled dimensions correspond to those for Specimen 1. The analyses found that the assumed value of Poisson's ratio had a significant effect on the computed deflections, but that the angle of twist had a small effect on the displacements along the center-line.

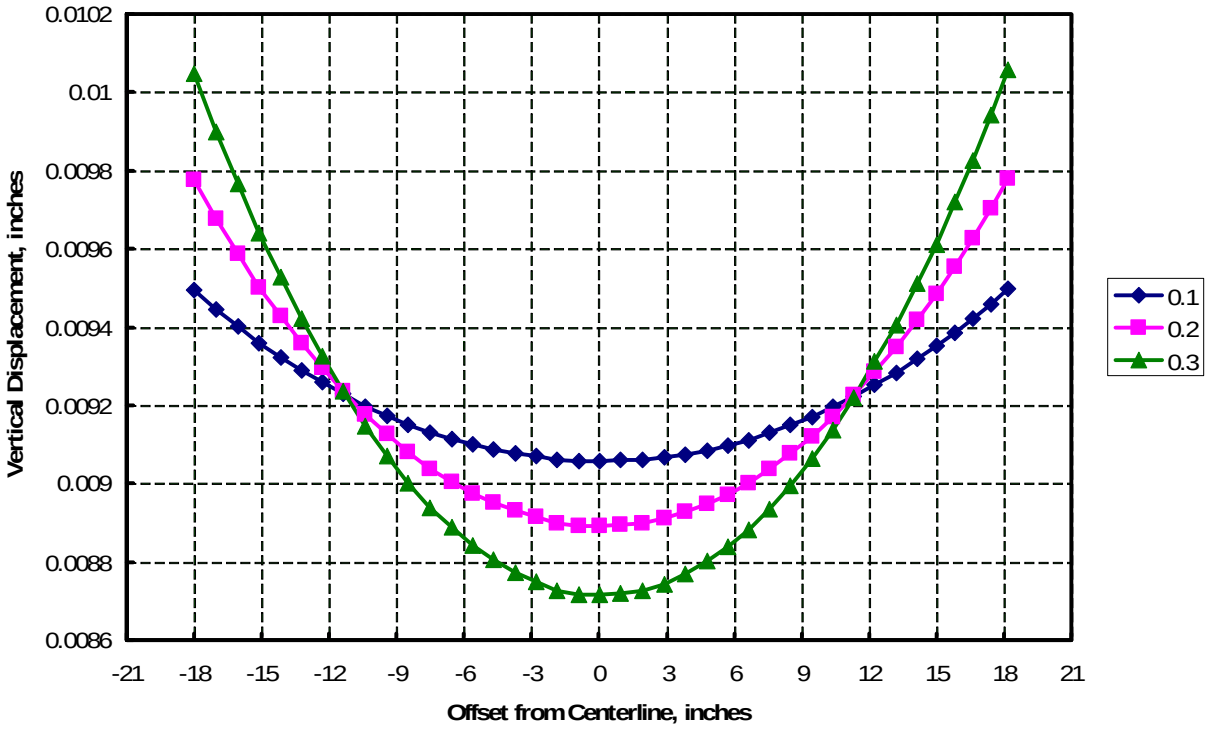

Figure A-1 Summary of Finite Element Models of Beam with Initial Twist, with Varying Values of Poisson's Ratio

Appendix B

Computation of Nonlinear Bending Stiffness and Moment Capacity[1]

Introduction

Application

The designer of deep foundations under lateral loading must make computations to ascertain that three factors of performance are within tolerable limits: combined axial and bending stress, shear stress, and pile-head deflection. The flexural rigidity, *EI*, of the deep foundation (bending stiffness) is an important parameter that influences the computations (Reese and Wang, 1988 Isenhower, 1994).

In general, flexural rigidity of reinforced concrete varies nonlinearly with the level of applied bending moment, and to employ a constant value of *EI* in the *p-y* analysis for a concrete pile will result in some degree of inaccuracy in the computations.

The response of a pile is nonlinear with respect to load because the soil has nonlinear stress-strain characteristics. Consequently, the load and resistance factor design (LRFD) method is recommended when evaluating piles as structural members. This requires evaluation of the nominal (i.e. unfactored) bending moment of the deep foundation.

Special features in LPile have been developed to compute the nominal-moment capacity of a reinforced-concrete drilled shaft, prestressed concrete pile, or steel-pipe pile and to compute the bending stiffness of such piles as a function of applied moment or bending curvature. The designer can utilize this information to make a correct judgment in the selection of a representative *EI* value in accordance with the loading range and can compute the ultimate lateral load for a given cross-section.

Assumptions

The program computes the behavior of a beam or beam-column. It is of interest to note that the *EI* of the concrete member will undergo a significant change in *EI* when tensile cracking occurs. In the coding used herein, the assumption is made that the tensile strength of concrete is minimal and that cracking will be closely spaced when it appears. Actually, such cracks will initially be spaced at some distance apart and the change in the *EI* will not be so drastic. In respect to the cracking of concrete, therefore, the *EI* for a beam will change more gradually than is given by the coding.

The nominal bending moment of a reinforced-concrete section in compression is computed at a compression-control strain limit in concrete of 0.003 and is not affected by the

---

[1] Contents of this Appendix are taken from Chapter 5 of the LPile 2012 Technical Manual by Isenhower and Wang.

crack spacing. The ultimate bending moment for steel, because of the large amount of deformation of steel when stressed about the proportional limit, is taken at a maximum strain of 0.015 which is five times that of concrete.

For reinforced-concrete sections in tension, the nominal moment capacity of a section is computed at a compression-control strain limit of 0.003 or a maximum tension in the steel reinforcement of 0.005.

Stress-Strain Curves for Concrete and Steel

Stress-Strain Curve for Unconfined Concrete

Any number of models can be used for the stress-strain curves for concrete and steel. For the purposes of the computations presented herein, some relatively simple curves are used. The stress-strain curve for concrete is shown in Figure B-1 (Hognestad, 1951).

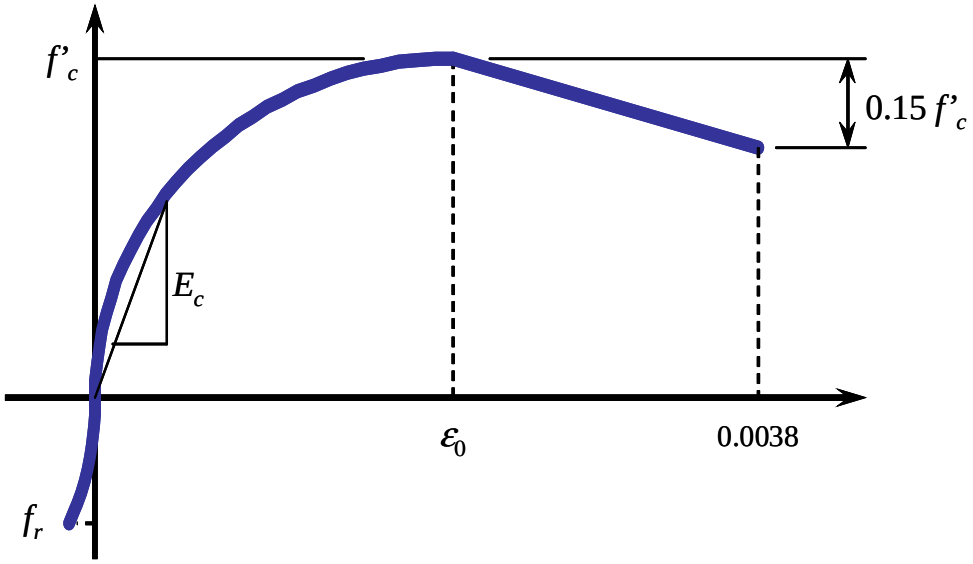

Figure B-1 Stress-Strain Relationship for Concrete Used by LPile

The following equations are used to compute concrete stress. The value of concrete compressive strength, f'_c, in these equations is specified by the engineer.

$$f_c = f'_c\left[2\frac{\varepsilon}{\varepsilon_0} - \left(\frac{\varepsilon}{\varepsilon_0}\right)^2\right] \text{ for } 0 \le \varepsilon \le \varepsilon_0 \quad \text{.....(B-1)}$$

$$f_c = f'_c - 0.15 f'_c\left(\frac{\varepsilon - \varepsilon_0}{0.0038 - \varepsilon_0}\right) \text{ for } \varepsilon_0 \le \varepsilon \le 0.0038 \quad \text{.....(B-2)}$$

The modulus of rupture, f_r, is the tensile strength of concrete in bending. The modulus of rupture for drilled shafts and bored piles is computed using

$$\begin{aligned} f_r &= 7.5\sqrt{f_c' \text{ psi}} \text{ in USCS units} \\ f_r &= 19.7\sqrt{f_c' \text{ kPa}} \text{ in SI units} \end{aligned} \quad \text{.....(B-3)}$$

The modulus of rupture for prestressed concrete piles is computed using

$$\begin{aligned} f_r &= 4.0\sqrt{f_c' \text{ psi}} \text{ in USCS units} \\ f_r &= 10.5\sqrt{f_c' \text{ kPa}} \text{ in SI units} \end{aligned} \quad \text{.....(B-4)}$$

The modulus of elasticity of concrete, E_c, is computed using

$$\begin{aligned} E_c &= 57{,}000\sqrt{f_c' \text{ psi}} \text{ in USCS units} \\ E_c &= 151{,}000\sqrt{f_c' \text{ kPa}} \text{ in SI units} \end{aligned} \quad \text{.....(B-5)}$$

The compressive strain at peak compressive stress, ε_0, is computed using

$$\varepsilon_0 = 1.7\frac{f_c'}{E_c} \quad \text{.....(B-6)}$$

Stress-Strain Curve for Confined Concrete

Concrete gain both strength and ductility in compression when confined by either casing or transverse reinforcing steel. The theoretical stress-strain curve developed by Mander, Priestley, and Park (1988) is used to compute the stress-strain curve for confined concrete.

Stress-Strain Curve for Steel

The stress-strain (σ-ε) curve for steel is shown in Figure B-2. There is no practical limit to plastic deformation in tension or compression. The stress-strain curves for tension and compression are assumed to be identical.

The yield strength of the steel, f_y, is selected according to the material being used, and the following equations apply.

$$\varepsilon_y = \frac{f_y}{E_s} \quad \text{.....(B-7)}$$

where E_s = 200,000 MPa or 29,000,000 psi

The models and the equations shown here are employed in the derivations that are shown subsequently.

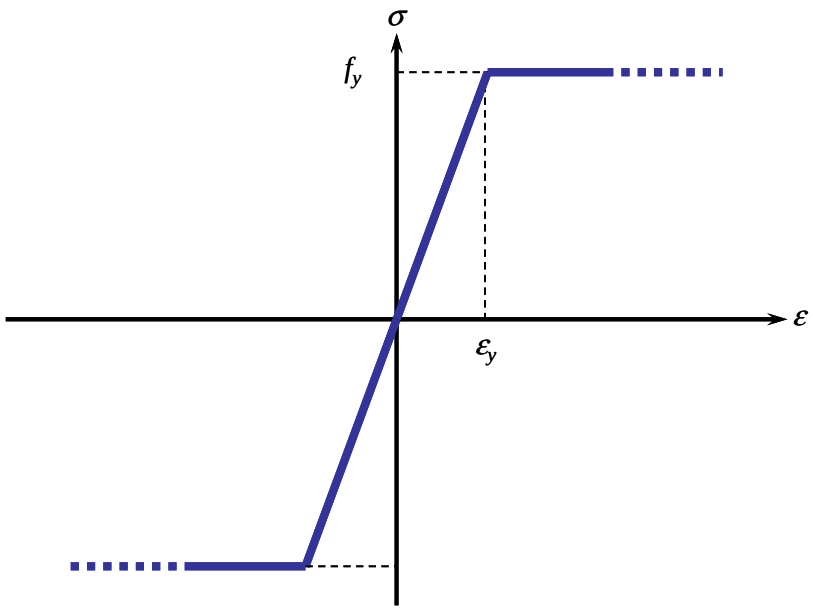

Figure B-2 Stress-Strain Relationship for Reinforcing Steel Used by LPile

Beam Theory

Flexural Behavior

The flexural behavior of a structural element such as a beam, column, or a pile subjected to bending is dependent upon its flexural rigidity, *EI*, where *E* is the modulus of elasticity of the material of which it is made and *I* is the moment of inertia of the cross section about the axis of bending. In some instances, the values of *E* and *I* remain constant for all ranges of stresses to which the member is subjected, but there are situations where both *E* and *I* vary with changes in stress conditions because the materials are nonlinear or crack.

The variation in bending stiffness is significant in reinforced concrete members because concrete is weak in tension and cracks and because of the nonlinearity in stress-strain relationships. As a result, the value of *E* varies; and because the concrete in the tensile zone below the neutral axis becomes ineffective due to cracking, the value of *I* is also reduced. When a member is made up of a composite cross section, there is no way to calculate directly the value of *E* for the member as a whole.

The following is a description of the theory used to evaluate the nonlinear moment-curvature relationships in LPile.

Consider an element from a beam with an initial unloaded shape of *abcd* as shown by the dashed lines in Figure B-3. This beam is subjected to pure bending and the element changes in shape as shown by the solid lines. The relative rotation of the sides of the element is given by the small angle $d\theta$ and the radius of curvature of the elastic element is signified by the length ρ measured from the center of curvature to the neutral axis of the beam. The bending strain ε_x in the beam is given by

$$\varepsilon_x = \frac{\Delta}{dx} \quad \text{.....(B-8)}$$

where:

Δ = deformation at any distance from the neutral axis, and

dx = length of the element along the neutral axis.

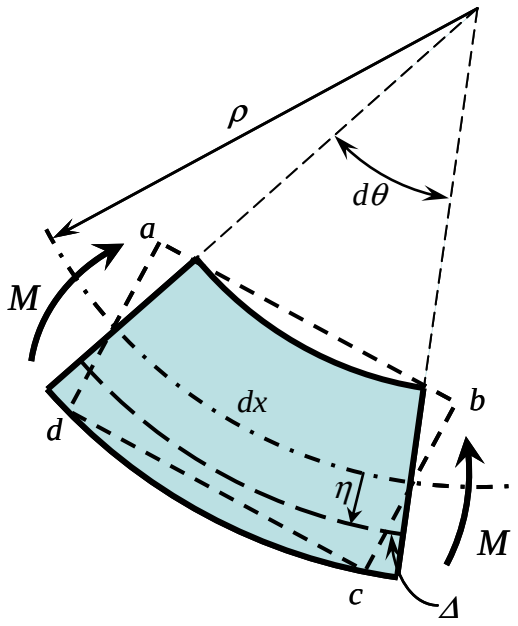

Figure B-3 Element of Beam Subjected to Pure Bending

The following equality is derived from the geometry of similar triangles

$$\frac{\rho}{dx} = \frac{\eta}{\Delta} \quad \text{.....(B-9)}$$

where:

η = distance from the neutral axis, and

ρ = radius of curvature.

Equation B-10 is obtained from Equations B-8 and B-9, as follows:

$$\varepsilon_x = \frac{\Delta}{dx} = \frac{\eta\, dx}{\rho}\,\frac{1}{dx} = \frac{\eta}{\rho} \quad \text{.....(B-10)}$$

From Hooke's Law

$$\sigma_x = E\varepsilon_x \quad \text{.....(B-11)}$$

where:

σ_x = unit stress along the length of the beam, and

E = Young's modulus.

Substituting Equation B-10 into Equation B-11, we obtain

$$\sigma_x = \frac{E\eta}{\rho} \quad \text{.....(B-12)}$$

From Euler-Bernoulli beam theory

$$\sigma_x = \frac{M\eta}{I} \quad \text{.....(B-13)}$$

where:

M = applied moment, and

I = moment of inertia of the section.

Equating the right sides of Equations B-12 and B-13, we obtain

$$\frac{M\eta}{I} = \frac{E\eta}{\rho} \quad \text{.....(B-14)}$$

Cancelling η and rearranging Equation B-14

$$\frac{M}{EI} = \frac{1}{\rho} \quad \text{.....(B-15)}$$

Continuing with the derivation, it can be seen that $dx = \rho\, d\theta$ and

$$\frac{1}{\rho} = \frac{d\theta}{dx} = \phi \quad \text{.....(B-16)}$$

For convenience here, the symbol ϕ is substituted for the curvature $1/\rho$. The following equation is developed from this substitution and Equations B-15 and B-16

$$EI = \frac{M}{\phi} \quad \text{.....(B-17)}$$

and because $\Delta = \eta\, d\theta$ and $\varepsilon_x = \Delta/dx$, we may express the bending strain as

$$\varepsilon_x = \phi\,\eta \quad \text{.....(B-18)}$$

The computation for a reinforced-concrete section, or a section consisting partly or entirely of a pile, proceeds by selecting a value of ϕ and estimating the position of the neutral axis. The strain at points along the depth of the beam can be computed by use of Equation B-18, which in turn will lead to the forces in the concrete and steel. In this step, the assumption is made that the stress-strain curves for concrete and steel are those shown.

With the magnitude of the forces, both tension and compression, the equilibrium of the section can be checked, taking into account the external compressive loading. If the section is not in equilibrium, a revised position of the neutral axis is selected and iterations proceed until the neutral axis is found.

Bending moment in the section is computed by integrating the moments of forces in the slices times the distances of the slices from the centroid. The value of *EI* is computed using Equation B-17. The maximum compressive strain in the section is computed and saved. The computations are repeated by incrementing the value of curvature until a failure strain in the concrete or steel pipe, is reached or exceeded. The nominal (unfactored) moment capacity of the section is found by interpolation using the values of maximum compressive strain.

Validation of Method

Analysis of Concrete Sections

An example concrete section is shown in Figure B-4. This rectangular beam-column has a cross section of 510 mm in width and 760 mm in depth and is subjected to both bending moment and axial compression. The compressive axial load is 900 kN. For this example, the compressive strength of the concrete f'_c is 27,600 kPa, *E* of the steel is 200 MPa, and the ultimate strength f_y of the steel is 413,000 kPa. The section has ten No. 25M bars, each with a cross-sectional area of 0.0005 m^2, and the row positions are shown in the Figure B-4. The following pages show how the values of *M* and *EI* as a function of curvature are computed.

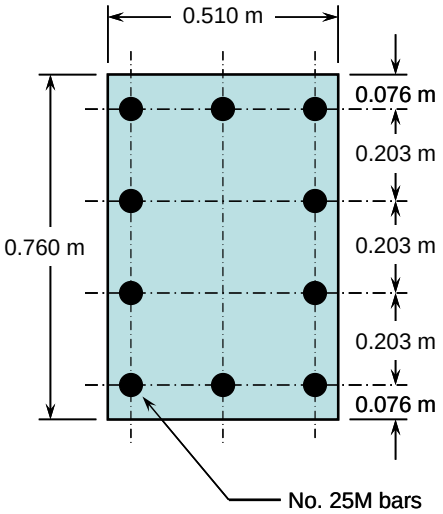

Figure B-4 Validation Problem for Mechanistic Analysis of Rectangular Section

The results from the solution of the problem by LPile are shown in Table B-1. The first block of lines include an echo-print of the input, plus several quantities computed from the input data, including the computed squash load capacity (9,093.096 kN), which is the load at which a short column would fail. The next portion of the output presents results of computations for various values of curvature, starting with a value of 0.0000492 rad/m and increasing ϕ by even increments.[2]

The fifth column of the output shows the value of the position of the neutral axis, as measured from the compression side of the member. Other columns in the output, for each value of ϕ, give the bending moment, the *EI*, and the maximum compressive strain in the concrete. For the validation that follows, only one line of output was selected.

Computations Using Equations of Section B-2

An examination of the output in Table B-1 finds that the maximum compressive strain was 0.0030056 for a value of ϕ of 0.0176673 rad/m. This maximum strain is close to 0.003, the value selected for computation of the nominal bending moment capacity, and that line of output was selected for the basis of the following hand computations.

Check of Position of the Neutral Axis

In Table B-1, the neutral axis is 0.1701205 m from the top of the section. The computer found this value by iteration by balancing the computed axial thrust force against the specified axial thrust. For the hand computations, the computed axial thrust for this neutral axis position will be checked against the specified axial thrust. In the hand computations, the value of the depth to the neutral axis was rounded to 0.1701 m for convenience.

Table B-1 LPile Output for Rectangular Concrete Section

```
--------------------------------------------------------------------------------
    Computations of Nominal Moment Capacity and Nonlinear Bending Stiffness
--------------------------------------------------------------------------------

Axial thrust values were determined from pile-head loading conditions


Number of Sections = 1


Section No. 1:


Dimensions and Properties of Rectangular Concrete Pile:

Length of Section                                =     15.24000000 m
Depth of Section                                 =      0.76000000 m
Width of Section                                 =      0.51000000 m
Number of Reinforcing Bars                       =              10 bars
Yield Stress of Reinforcing Bars                 =         413686. kPa
Modulus of Elasticity of Reinforcing Bars        =      199948000. kPa
Compressive Strength of Concrete                 =          27600. kPa
Modulus of Rupture of Concrete                   =    -39.40177573 kPa
Gross Area of Pile                               =      0.38760000 sq. m
Total Area of Reinforcing Steel                  =      0.00500000 sq. m
Area Ratio of Steel Reinforcement                =      1.28998971 percent
Nom. Axial Structural Capacity = 0.85 Fc Ac + Fs As  =        9093.096 kN

Reinforcing Bar Details:
```

[2] LPile uses an algorithm to compute the initial increment of curvature that is based on the depth of the pile section. This algorithm is designed to obtain initial values of curvature small enough to capture the uncracked behavior for all pile sizes.

Bar Number	Bar Index	Bar Diam. m	Bar Area sq. m	Bar X m	Bar Y m
1	16	0.025200	0.000500	-0.167500	0.304800
2	16	0.025200	0.000500	0.000000	0.304800
3	16	0.025200	0.000500	0.167500	0.304800
4	16	0.025200	0.000500	-0.167500	0.101600
5	16	0.025200	0.000500	0.167500	0.101600
6	16	0.025200	0.000500	-0.167500	-0.101600
7	16	0.025200	0.000500	0.167500	-0.101600
8	16	0.025200	0.000500	-0.167500	-0.304800
9	16	0.025200	0.000500	0.000000	-0.304800
10	16	0.025200	0.000500	0.167500	-0.304800

Concrete Properties:

```
Compressive Strength of Concrete                    =         27600. kPa
Modulus of Elasticity of Concrete                   =      24865024. kPa
Modulus of Rupture of Concrete                      =  -3271.7136591 kPa
Compression Strain at Peak Stress                   =      0.0018870
Tensile Strain at Fracture                          =     -0.0001154
Maximum Coarse Aggregate Size                       =      0.0190500 m
```

Number of Axial Thrust Force Values Determined from Pile-head Loadings = 1

Number	Axial Thrust Force kN
1	900.000

Definitions of Run Messages and Notes:

```
   C = concrete has cracked in tension
   Y = stress in reinforcement has reached yield stress
   T = tensile strain in reinforcement exceeds 0.005 when compressive strain
       in concrete is less than 0.003.
   Bending stiffness = bending moment / curvature
   Position of neutral axis is measured from compression side of pile
   Compressive stresses are positive in sign. Tensile stresses are negative in sign.
```

Axial Thrust Force = 900.000 kN

Bending Curvature rad/m	Bending Moment kN-m	Bending Stiffness kN-m2	Depth to N Axis m	Max Comp Strain m/m	Max Tens Strain m/m	Max Concrete Stress kPa	Max Steel Stress kPa	Run Msg
0.0000492	28.3173948	575409.	1.9085538	0.0000939	0.0000565	2674.0029283	18743.	
0.0000984	56.6333321	575395.	1.1451716	0.0001127	0.0000379	3188.4483827	22462.	
.								
. (deleted lines)								
.								
0.0004429	253.1619332	571583.	0.5542915	0.0002455	-0.0000911	6671.6631466	48751.	
0.0004921	280.6180646	570216.	0.5375669	0.0002646	-0.0001095	7149.3433542	52522.	
0.0005413	280.6180646	518378.	0.4727569	0.0002559	-0.0001555	6926.7437852	50760.	C
0.0005906	280.6180646	475180.	0.4548249	0.0002686	-0.0001802	7241.7196541	53257.	C
.								
. (deleted lines)								
.								
0.0038878	651.6508321	167614.	0.2450564	0.0009527	-0.0020020	20619.	-397341.	C
0.0039862	663.0531399	166336.	0.2440064	0.0009727	-0.0020569	20904.	-408237.	C
0.0040846	674.4235902	165112.	0.2430210	0.0009927	-0.0021117	21183.	-413686.	CY
0.0041831	685.7618089	163937.	0.2420960	0.0010127	-0.0021664	21458.	-413686.	CY
.								
. (deleted lines)								
.								
0.0176673	**907.1915259**	**51349.**	**0.1701205**	**0.0030056**	**-0.0104216**	**27596.**	**413686.**	**CY**
.								
. (deleted lines)								
.								
0.0239665	913.9027316	38132.	0.1658249	0.0039742	-0.0142403	27600.	413686.	CY

Summary of Results for Nominal (Unfactored) Moment Capacity for Section 1

Moment values interpolated at maximum compressive strain = 0.003
or maximum developed moment if pile fails at smaller strains.

Load No.	Axial Thrust kN	Nominal Mom. Cap. kN-m	Max. Comp. Strain
1	900.000	907.021	0.00300000

```
Note note that the values of moment capacity in the table above are not
factored by a strength reduction factor (phi-factor).

In ACI 318-08, the value of the strength reduction factor depends on whether the
transverse reinforcing steel bars are spirals or tied hoops.

The above values should be multiplied by the appropriate strength reduction
factor to compute ultimate moment capacity according to ACI 318-08, Section 9.3.2.2
or the value required by the design standard being followed.
```

Forces in Reinforcing Steel

The rows of steel in Figure B-4 are numbered from the top downward. Therefore, Row 1 will be in compression and the other rows will be in tension. The strain in each row of bars is computed using Equation B-18, as follows (with the positive sign indicating compression).

$$\varepsilon_1 = \phi\,\eta = (0.0176673 \text{ rad/m})\,(0.1701 \text{ m} - 0.0755 \text{ m}) = +0.001672$$

Similarly,

$\varepsilon_2 = -0.001915$

$\varepsilon_3 = -0.005501$

$\varepsilon_4 = -0.009088$

In order to obtain the forces in the steel at each level, it is necessary to know if the steel is in the elastic or plastic range. Thus, it is required to compute the value of yield strain ε_y using Equation B-7.

$$\varepsilon_y = \frac{f_y}{E_s} = \frac{413{,}000}{2\times10^8} = 0.002065 \quad \text{.....(B-19)}$$

This computation shows that the bars in rows 1 and 2 are in the elastic range and the bars in the other two rows are in the plastic range. Thus, the forces in each row of bars are:

F_1 = (3 bars) $(5 \times 10^{-4}$ m^2/bar) (0. 001447) $(2 \times 10^8$ kPa) = 501.51 kN

F_2 = (2 bars) $(5 \times 10^{-4}$ m^2/bar) (–0. 002779) $(2\times10^8$ kPa) = –382.95 kN

F_3 = (2 bars) $(5 \times 10^{-4}$ m^2/bar) (–0.007005) (413,000 kPa) = –413.00 kN

F_4 = (3 bars) $(5 \times 10^{-4}$ m^2/bar) (–0.007005) (413,000 kPa) = –619.50 kN

Total of forces in the reinforcing bars = –913.95 kN.

Forces in Concrete

In computing the internal force in the concrete, 10 slices that are 17.01 mm (0.670 in.) in thickness are selected for computation of the 0.1701 m of the section in compression. The slices

are numbered from the top downward for convenience. The strain is computed at the mid-height of each slice by making use of Equation B-18.

$$\varepsilon_1 = \phi\,\eta = (0.0176673 \text{ rad/m})\ (0.1701 \text{ m} - 0.01701 \text{ m}/2) = 0.00285529$$

The second value in the parentheses is the distance from the neutral axis to the mid-height of the first slice. Similarly, the strains at the centers of the other slices are:

$\varepsilon_2 = 0.002554$

$\varepsilon_3 = 0.002254$

$\varepsilon_4 = 0.001954$

$\varepsilon_5 = 0.001653$

$\varepsilon_6 = 0.001353$

$\varepsilon_7 = 0.001052$

$\varepsilon_8 = 0.000751$

$\varepsilon_9 = 0.000451$

$\varepsilon_{10} = 0.000150$

The forces in the concrete are computed by employing Figure B-4 and Equations B-1 through B-7. The first step is to compute the value of ε_0 from Equation B-6 and to see the strains are lower or greater than the strain for the peak stress.

$$\varepsilon_0 = 1.7\left(\frac{27{,}600}{151{,}000\sqrt{27{,}600}}\right) = 0.001870$$

The strain in the top two slices show that stress can be found by use of the second branch of the compressive portion of the curve in Figure B-4 and the stress in the other slices can be computed using Equation B-1. From Figure B-4, the following quantity is computed

$$0.15\,f_c' = 4{,}140 \text{ kPa}$$

Then, the following equation can be used to compute the stress along the descending section of the stress-strain curve corresponding to ε_1 and ε_2.

$$f_c = 27{,}600 - 4{,}140\left(\frac{\varepsilon - 0.001870}{0.0038 - 0.001870}\right)$$

From the above equation:

f_{c1} = 25,487 kPa

f_{c2} = 26,132 kPa

f_{c3} = 26,777 kPa

f_{c4} = 27,421 kPa

The strains in the other slices are less than ε_0 so the stresses in the concrete are on the ascending section of the stress-strain curve. The stresses in these slices can be computed by Equation B-1.

$$f_{c3} = 27{,}600\left[2\left(\frac{\varepsilon}{0.001870}\right)-\left(\frac{\varepsilon}{0.001870}\right)^2\right]$$

The other values of f_c are computed as follows:

f_{c5} = 27,227 kPa

f_{c6} = 25,484 kPa

f_{c7} = 22,315 kPa

f_{c8} = 17,721 kPa

f_{c9} = 11,702 kPa

f_{c10} = 4,257 kPa

The forces in each slice of the concrete due to the compressive stresses are computed by multiplying the area of the slice by the computed stress. All of the slices have the area of 0.00740 m^2 (0.0145 m $\times$ 0.51 m). Thus, the computed forces in the slices are:

F_{c1} = 221.13 kN

F_{c2} = 226.72 kN

F_{c3} = 232.32 kN

F_{c4} = 237.91 kN

F_{c5} = 236.23 kN

F_{c6} = 221.10 kN

F_{c7} = 193.61 kN

F_{c8} = 153.75 kN

F_{c9} = 101.53 kN

F_{c10} = 36.93 kN

There is a small section of concrete in tension. The depth of the tensile section is determined by the strains up to the strain developed at the modulus of rupture (Equation B-3).

$$f_r = 19.7\sqrt{27{,}600} = -3{,}273 \text{ kPa}$$

In this zone, it is assumed that the stress-stain curve in tension is defined by the average concrete modulus (Equation B-5).

The modulus of elasticity of concrete, E_c, is computed using

$$E_c = 151{,}000\sqrt{27{,}600} = 25{,}086{,}000 \text{ kPa}$$

The strain at rupture is then

$$\varepsilon_r = \frac{-3{,}273}{25{,}086{,}000} = -0.0001305$$

The thickness of the tension zone is computed using Equation B-18 as

$$h = \frac{\varepsilon_r}{\phi} = \frac{-0.0001305}{0.0176673} = -0.07384 \text{ m}$$

The force in tension is the product of average tensile stress is and the area in tension and is

$$F_t = \left(\frac{\varepsilon_r E_c}{2}\right)(0.07384)(0.510) = -6.16 \text{ kN}$$

A reduction in the computed concrete force is needed because the top row of steel bars is in compression zone. The compressive force computed in concrete for the area occupied by the steel bars must be subtracted from the computed value. The compressive strain at the location of the top row of bars is 0.001447, the area of the bars is 0.0015 m^2, the concrete stress is 27,289 kPa, and the force is 40.93 kN.

Thus, the total force carried in the concrete is sum of the computed compressive forces plus the tensile concrete force minus the correction for the area of concrete occupied by the top row of reinforce is 1814.10 kN.

Computation of Balance of Axial Thrust Forces

The summation of the internal forces yields the following expression for the sum of axial thrust forces:

$$\Sigma F = 1814.10 \text{ kN} - 913.95 \text{ kN} = 900.15 \text{ kN}.$$

Taking into account the applied axial load in compression of 900 kN, the section is out of balance by only 0.15 kN (33.7 lbs).

This hand computation confirms the validity of the computations made by LPile. The selection of a thickness of the increments of concrete of 0.01701 m is thicker than that used in LPile. LPile uses 100 slices of the full section depth in its computations, so the slice thickness used by LPile is 0.0076 m for this example problem. Also, some error was introduced by the reduced precision in the hand computations, whereas LPile uses 64-bit precision in all computations.

Computation of Bending Moment and *EI*

Bending moment is computed by summing the products of the slice forces about the centroid of the section. The axial thrust load does not cause a moment because it is applied with no eccentricity. The moments in the steel bars and concrete can be added together because the bending strains are compatible in the two materials.

The moments due to forces in the steel bars are computed by multiplying the forces in the steel bars times the distances from the centroid of the section. The values of moment in the steel bars are:

Moment due to bar row 1: (479.1 kN) (0.3045) =	152.71 kN-m
Moment due to bar row 2: (–411.9 kN) (0.1015) =	–38.87 kN-m
Moment due to bar row 3: (–415.0 kN) (–0.1015) =	41.92 kN-m
Moment due to bar row 4: (–622.5 kN) (–0.3045) =	188.64 kN-m
Total moment due to stresses in steel bars =	344.40 kN-m

The moments due to forces in the concrete are computed by multiplying the forces in the concrete times the distances from the centroid of the section. The values of moments in the concrete slices are:

Moment in slice 1: (241.37 kN) (0.3728 m) =	82.15 kN-m
Moment in slice 2: (248.29 kN) (0.3583 m) =	80.37 kN-m
Moment in slice 3: (255.21 kN) (0.3438 m) =	78.40 kN-m
Moment in slice 4: (257.61 kN) (0.3293 m) =	76.24 kN-m
Moment in slice 5: (247.22 kN) (0.3148 m) =	71.68 kN-m
Moment in slice 6: (226.19 kN) (0.3003 m) =	63.33 kN-m
Moment in slice 7: (194.53 kN) (0.2858 m) =	52.16 kN-m

Moment in slice 8: (152.24 kN) (0.2713 m) = 38.81 kN-m

Moment in slice 9: (99.32 kN) (0.2568 m) = 23.90 kN-m

Moment in slice 10: (35.76 kN) (0.2423 m) = 8.07 kN-m

Moment correction for top row of steel bars = (–40.93 kN) (0.3045 m) = –12.46 kN-m

Total moment due to stresses in concrete = 561.32 kN-m.

Sum of moments in steel bars and concrete = 905.71 kN-m.

As mentioned above, the summation of the moments in the steel bars and concrete is possible because the bending strains in the two materials are compatible, i.e. the bending strains are consistent with the positions of the steel bars and concrete slices.

Computation of Bending Stiffness Using Approximate Method

The drawing in Figure B-5 shows the information used in computing the nominal moment capacity. The forces in the steel were computed by multiplying the stress developed in the steel by the area, for either of two or three bars in a row at each row position.

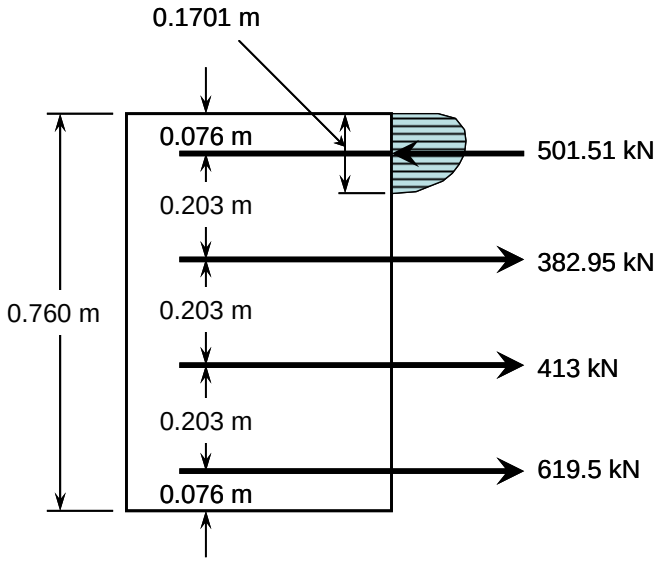

Figure B-5 Free Body Diagram Used for Computing Nominal Moment Capacity of Reinforced Concrete Section

The value of bending stiffness is computed using Equation B-17.

$$EI = \frac{M}{\phi} = \frac{905.71\,\text{kN - m}}{0.01701205\,\text{rad/m}} = 51.265.02\,\text{kN - m}^2$$

A comparison of results from hand versus computer solutions is summarized in Table B-2. The moment computed by LPile was 907.19 kN-m. Thus, the hand calculation is within 0.16%

of the computer solution. The value of the *EI* is computed by LPile is 51,348.62 kN-m^2. The hand solution is within 0.16% of the computer solution. The hand solution for axial thrust is within 0.0-2% of the computer solution

The agreement is close between the values computed by hand using only a small number of slices and the values from the computer solution computed using 100 slices. This example hand computation serves to confirm of the accuracy of the computer solution for the problem that was examined.

Table B-2 Comparison of Results from Hand Computation vs. Computer Solution

Parameter	By LPile	By Hand	Hand Error, %
Moment Capacity, kN-m	907.19	905.71	–0.16%
Bending Stiffness, *EI*, kN-m^2	51,348.62	51,265.02	–0.16%
Axial Thrust, kN	900.00*	900.15	+0.02%

* Input value

The rectangular section used for above example solution was chosen because the geometric shapes of the slices are easy to visualize and their areas and centroid positions are easy to compute. In reality, the algorithms used in LPile for the geometrical computation are much more powerful because of the circular and non-circular shapes considered in the computations. For example, when a large number of slices are used in computations, individual bars are divided by the slice boundaries. So, in the computations by LPile, the areas and centroidal positions of the circular segments of bars are computed. In addition, the areas of bars and strands in a slice are subtracted from the area of concrete in a slice.

The two following graphs are examples of the output from LPile for curves of moment versus curvature and ending stiffness versus bending moment. These graphs are examples of the output from the presentation graphics utility that is part of LPile. Both of these graphs were exported as enhanced Windows metafiles, which were then pasted into this document.

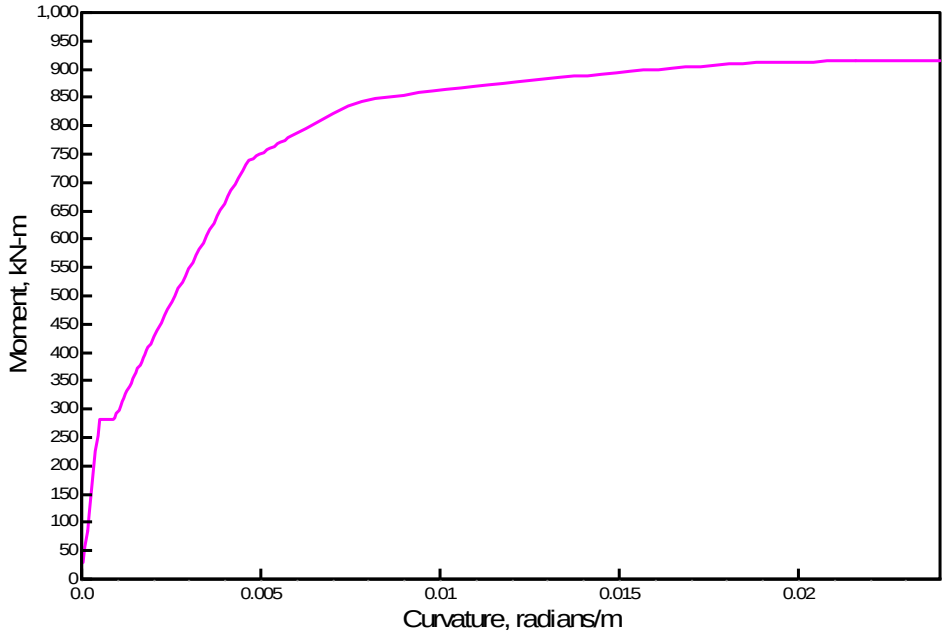

Figure B-6 Moment vs. Curvature

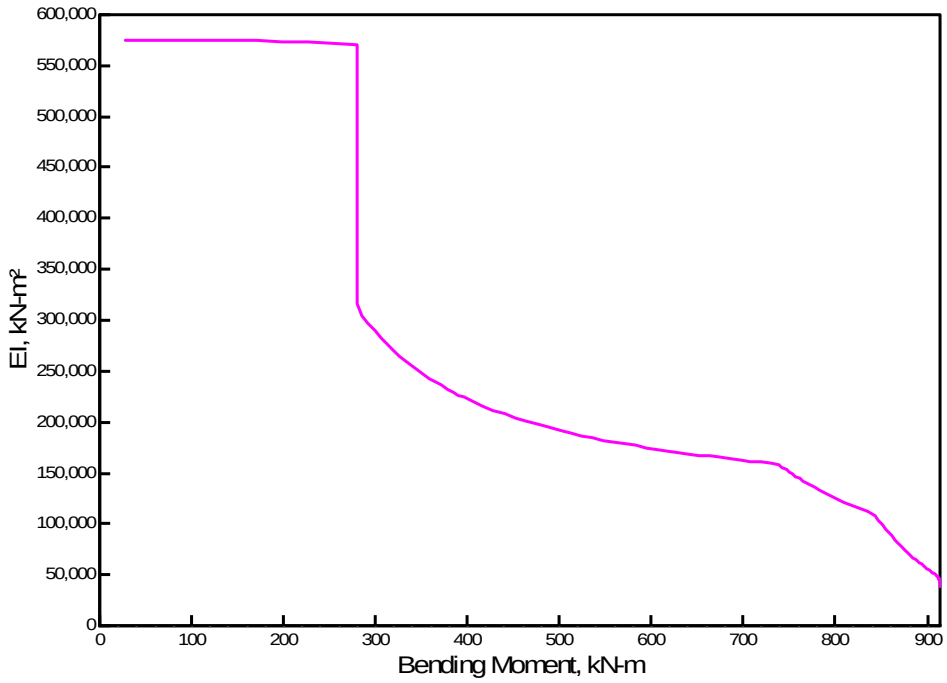

Figure B-7 Bending Moment vs. Bending Stiffness

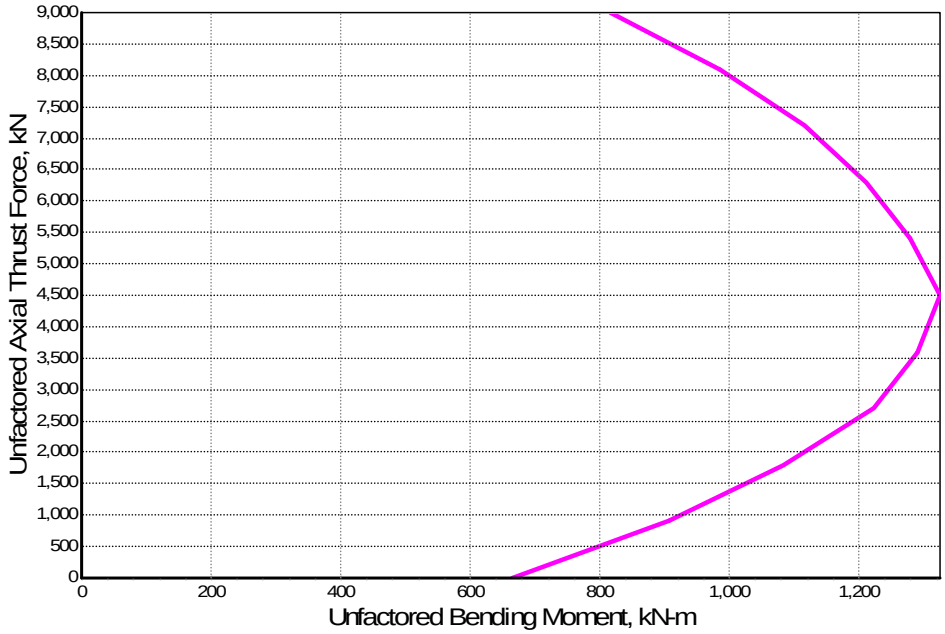

Figure B-8 Interaction Diagram for Nominal Moment Capacity

References

Architectural Testing, Inc., 2012. Performance Test Report (Draft), Report No. B7179.01-122-42, 17 p.

Architectural Testing, Inc., 2012. Performance Evaluation Test Report (Draft), Product Concrete Report No. B7179.01-122-31, 4 p.

Architectural Testing, Inc., 2012. Performance Evaluation Test Report (Draft), Product Steel Reinforcement Bar, Report No. B7179.01-122-31, 3 p.

Hognestad, E. 1951. *A Study of Combined Bending and Axial Load in Reinforced Concrete Members*, Bulletin 339. University of Illinois Engineering Experiment Station, Urbana, Illinois, June, 128 p.

Isenhower, W. M., 1994. "Improved Methods for Evaluation of Bending Stiffness of Deep Foundations," *Proceedings*, Intl. Conf. on Design and Construction of Bridge Foundations, Vol. 2, pp. 571-585.

Isenhower, W. M., and Wang, S.-T., 2012. *Technical Manual for LPile 2012-06*, Ensoft, Inc., Austin, Texas.

Mander, J. B.; Priestley, M. J. N.; and Park, R., 1988. "Theoretical Stress-Strain Model for Confined Concrete," *Journal of Structural Engineering*, ASCE, Vol. 114, No. 8, pp. 1804-1826.

Reese, L. C., and Wang, S.-T. 1988. "The Effect of Nonlinear Flexural Rigidity on the Behavior of Concrete Piles Under Lateral Loading," *Texas Civil Engineer*, May, pp. 17-23.